

## 3D Measuring and Marking System for Building Equipment: Developing and Evaluating Prototypes

Shintaro Sakamoto, Hiroki Kishimoto, Kouetu Tanaka and Yukiteru Maeda

Research and Development Center, Shinryo Corporation, 41 Wadai, Tsukuba, Ibaraki, 300-4247, Japan, PH 81 298 64 6105; Fax 81 298 64 6127; e-mail:sakamoto.sh@shinryo.com

### **Abstract**

The measuring work has been done manually with the scales in the construction of building equipments. We have been studying a 3D measuring and marking system using a total station to increase accuracy and decrease workload. One feature is the pointing device for measuring indirectly the hidden areas which cannot be measured with a stand-alone total station. The device has a sensor which consists of a pinhole and a position sensitive detector for measuring the incident angles of the received laser and it's possible to calculate the pointing position by using the data. The other is the positioning device for marking accurately relative to the points which the total station indicates with the laser automatically. The displacement from the target position is calculated from the device position and the operator marks with the marking position adjusting function of the device. This paper describes the system configuration, measuring and marking theory of the system with those devices, and the results of evaluation experiments with prototypes.

**Keywords:** Building Equipment, 3D Position Measuring and Marking System, Total Station, Position Sensitive Detector

### **1. Introduction**

In the construction of air-conditioning systems, the position of system elements is marked out on structures such as floors and ceilings by measuring the distance from the datum line of the building with reference to the drawings. In renewal projects, construction planning is based on the measurement data of the existing equipment. Conventionally, these measurements represent two-dimensional distance data obtained using a scale or a compact laser range finder. It is considered that a shift to 3D coordinate measurement and seamless connection of a 3D CAD system and on-site measuring system will significantly improve the accuracy of measuring and the efficiency of work, concretely, decreasing the rework substantially.

Indoor 3D measuring methods based on the principle of GPS have been proposed in the past but these have lacked sufficient accuracy for position measurement in construction applications. Additionally, they are inadequate for marking applications because they cannot locate target positions directly to the site. In more recent years, instruments that measure 3D coordinates by measuring distance and angle, such as laser scanners and total stations, have been used in construction fields. But because they need to be moved to measure the positions in hidden areas, they tend to increase the workload and lower accuracy through the frequent displacement, because most points of measurement in equipment work are in a crowded location, a machine room, for example. And a laser scanner is impractical for acquiring measuring data on-site because of the specialized technique required and because several million sets of point data have to be processed. In marking work, compensation for the irradiating position is necessary because the positions depend on the accuracy of structures such as the floor, walls and ceiling. In addition, laser spot stretching because of slanting decreases marking accuracy.

In this research, we have developed a 3D measuring system for equipment work. The system consists of a total station, a pointing device for indirect measurement of the position in hidden areas and a positioning device for improving marking accuracy. This paper will show the configuration, system usage, and the mechanism and measuring principles of each device. Also, it will show the results of evaluation experiments using a prototype of the system.

## 2. System Configuration and Modes of Operation

This system is based on the total station concept and comprises a pointing device, positioning device and a host PC. The total station is a Leica Geosystems TCRP1205+. The accuracy of angle measurements is 5 seconds and distance accuracy is 1 mm + 1.5 ppm in the prism mode and 2 mm + 2 ppm in the non-prism mode.

This system has three operational modes: an initializing mode, position measurement mode, and positioning mode. The initializing mode is used to measure the self-position of the total station with reference to the datum line of the building or two points whose coordinates are known. The reference points are measured by setting a prism on them. The position measurement mode is used for measuring the 3D coordinates of not only the point collimated directly but also the hidden point with the pointing device. In the case of using the device, the operator establishes contact between the tip of the device and the objective position, and then adjusts the device posture as the laser is irradiated to the appropriate position. The total station measures the device position and the device measures the laser incident angles and the rotational angle around the laser. The system calculates the 3D coordinates of the pointed position with those measurement values. In the positioning mode, the total station irradiates the laser to the target position input to the system preliminarily or on site. After setting the positioning device on the position, the system measures the distance and the angles to the prism on the device. The displacement from the target position is calculated and shown to the operator. The operator marks referring the value.

## 3. Pointing Device

### 3.1 Angle Parameter of Device

As shown in Figure 1, the position of the laser receiving point P0 is measured directly on  $\Sigma_1$  whose origin is the position of the Total Station. The posture of the device is determined by the rotational angle around the laser axis and the laser incident angles. The local coordinate system of the device  $\Sigma_2$  is defined as the origin is P0, the z axis is conformed to the laser direction and the x axis is on the vertical plane. The rotational angle around the z axis is defined as  $\gamma$ , the angle of the laser incident direction is  $\alpha$  and the angle between the laser and the normal vector of the receiving surface is  $\beta$  on  $\Sigma_2$  as shown in Figure 2. The coordinates of the pointing position are calculated by these three angles.

### 3.2 Laser Incident Angle Sensor

The device has an angle sensor composed of the pinhole and position-sensitive detector or PSD, for measuring the angle of  $\alpha$  and  $\beta$ . PSD is the sensor which detects the position of the light spot via the surface resistance of the photodiode, a 2D PSD "S1880" produced by Hamamatsu Photonics, shown in Figure 3. As shown in Figure 4, when the laser is irradiated to the pinhole, the laser which passes through the pinhole is irradiated to the PSD as laser spot S. Because its position depends on the angle of  $\alpha$  and  $\beta$ , it is possible to measure them from the position of S. Here,  $\alpha$  is defined as the angle from the x axis of PSD and calculated using the following equation:

$$\cos\alpha = x_p / r, \text{ where } S = S(x_p, y_p) \text{ and } r = \sqrt{x_p^2 + y_p^2} \quad (\text{Eq. 1})$$

$\beta$  is expressed as the function of the length r shown in equation 1 and is constantly plus. The incident angle sensor is a modular structure and is demountable from the device, enabling it to be set to calibration equipment as shown in Figure 5. Using this equipment, the calibration curve of  $\beta$  is obtained from data r and the inclination angle of the sensor module by a least square method, as shown in Figure 6. Also, the offset values depending on the mechanical accuracy of PSD and its embedding are measuring with this equipment.

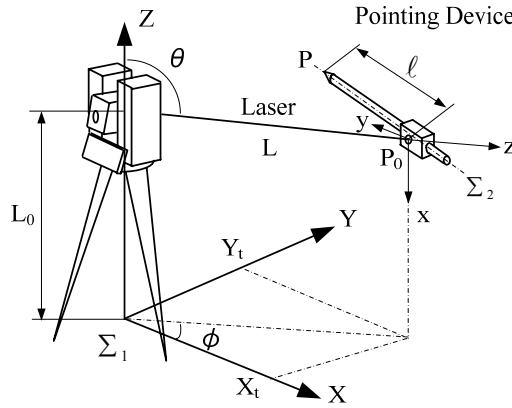


Figure 1 Definition of Coordinates

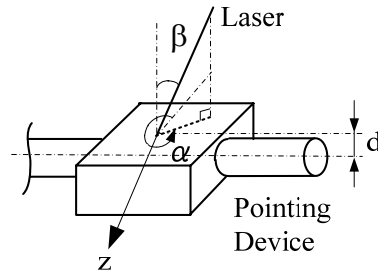


Figure 2 Definition of  $\alpha, \beta$

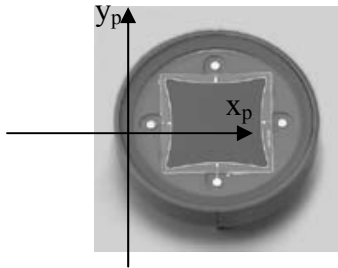


Figure 3 Position Sensitive Detector (PSD)

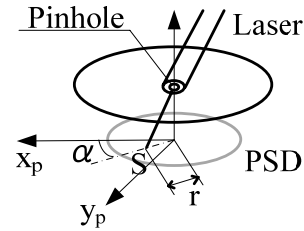


Figure 4 Measurement of  $\alpha, \beta$

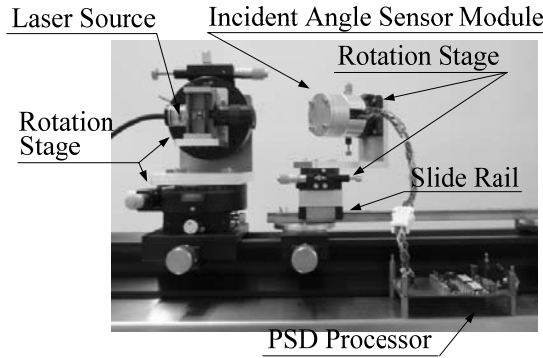


Figure 5 Calibration Equipment

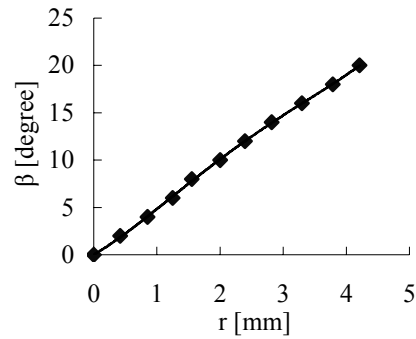


Figure 6 Calibration Curve of  $\beta$

### 3.3 Measurement of $\gamma$

The rotational angle  $\gamma$  around the z axis on the device coordinates system is measured using the inclinometer embedded parallel to the laser receiving surface. It enables angle measurement of 360 degrees. The resolution is 0.00549 degree and the linearity  $\pm 0.2$  degree. However,  $\gamma$  cannot be measured directly by the sensor because the sensor's measurement value is affected by  $\alpha, \beta$  and the vertical angle of P0  $\theta$ , shown in Figure 1. Therefore,  $\gamma$  is measured indirectly using the fact that the angle  $\varphi$  between the vector  $\vec{M}$ , meaning the basic axis of the inclinometer, which is transformed by  $\alpha, \beta, \gamma$  and  $\theta$ , and the vector  $\vec{G}$ , meaning the axis of the gravity orthographically projected to the laser receiving surface, are equal to the measurement value of the inclinometer. The angle  $\varphi$  is found by the following equation.

$$\cos \varphi = \vec{M} \cdot \vec{G} / \|\vec{M}\| \cdot \|\vec{G}\| \quad (\text{Eq. 2})$$

The vector  $\bar{M}$  is obtained by translating the vector of the basic axis of the inclinometer on  $\Sigma_2$ ,  $\bar{m} = [1, 0, 0]^T$ , as the following. Here, the trigonometric function of cosine and sine are shown in the abbreviation as C and S.

(1) Rotation by  $\gamma$

$$\bar{m}' = \begin{bmatrix} C_\gamma & -S_\gamma & 0 \\ S_\gamma & C_\gamma & 0 \\ 0 & 0 & 1 \end{bmatrix} \cdot \bar{m} = \begin{bmatrix} C_\gamma \\ S_\gamma \\ 0 \end{bmatrix} \quad (\text{Eq. 3})$$

(2) Transform by  $\alpha$  and  $\beta$

As shown in Figure 7, the transform by  $\alpha$  and  $\beta$  is equal to the transform of rotating in  $\Sigma_2$  around the vector  $\bar{\omega} = [S(\alpha - \gamma), C(\alpha - \gamma), 0]^T$ .

$$\bar{m}'' = (\bar{m}' \cdot \bar{\omega}) \cdot \bar{\omega} + C_\beta \{ \bar{m}' - (\bar{m}' \cdot \bar{\omega}) \cdot \bar{\omega} + S_\beta (\bar{\omega} \times \bar{m}') \} = \begin{bmatrix} S_\alpha S_{\alpha-\gamma} + C_\beta (C_\gamma - S_\alpha S_{\alpha-\gamma}) \\ S_\alpha C_{\alpha-\gamma} + C_\beta (S_\gamma - S_\alpha C_{\alpha-\gamma}) \\ -C_\alpha S_\beta \end{bmatrix} \quad (\text{Eq. 4})$$

(3) Rotation by  $\theta$

$$\bar{M} = \begin{bmatrix} C_\theta & 0 & S_\theta \\ 0 & 1 & 0 \\ -S_\theta & 0 & C_\theta \end{bmatrix} \cdot \bar{m}'' = \begin{bmatrix} C_\theta \{ S_\alpha S_{\alpha-\gamma} + C_\beta (C_\gamma - S_\alpha S_{\alpha-\gamma}) \} - S_\theta C_\alpha S_\beta \\ S_\alpha C_{\alpha-\gamma} + C_\beta (S_\gamma - S_\alpha C_{\alpha-\gamma}) \\ -S_\theta \{ S_\alpha S_{\alpha-\gamma} + C_\beta (C_\gamma - S_\alpha S_{\alpha-\gamma}) \} - C_\theta C_\alpha S_\beta \end{bmatrix} \quad (\text{Eq. 5})$$

The vector  $\bar{G}$  is obtained by translating the gravity vector  $\bar{g} = [0, 0, -1]^T$  with the orthographical projection matrix Q derived from the direction cosine of the receiving surface. The direction cosine is derived by the same translation of the vector  $\bar{n} = [0, 0, 1]^T$  as the vector  $\bar{M}$  with equations 1, 2 and 3. The vector  $\bar{G}$  is expressed as equation 6.

$$\bar{G} = \mathbf{Q} \cdot \bar{g} = \begin{bmatrix} (C_\theta S_\beta C_{\alpha-\gamma} + S_\theta C_\beta) \cdot (C_\theta C_\beta - S_\theta S_\beta C_{\alpha-\gamma}) \\ -S_\beta S_{\alpha-\gamma} (C_\theta C_\beta - S_\theta S_\beta C_{\alpha-\gamma}) \\ (C_\theta C_\beta - S_\theta S_\beta C_{\alpha-\gamma})^2 - 1 \end{bmatrix} \quad (\text{Eq. 6})$$

### 3.4 Derivation of Pointing Coordinate

As shown in Figures 1 and 2, the Total Station height is described as L0, the distance to the receiving surface is L, the horizontal angle is  $\phi$  and the vertical angle is  $\theta$  on  $\Sigma_1$ . When the axial length between P0 and P is described as  $\ell$  and the offset of the thickness direction is d, the pointing position P[0,  $\ell$ , d] is translated to P'' with equations 3 and 4.

$$\mathbf{P}'' = \begin{bmatrix} P_1 \\ P_2 \\ P_3 \end{bmatrix} = \begin{bmatrix} C_\alpha S_{\alpha-\gamma} \ell - C_\beta (S_\gamma + C_\alpha S_{\alpha-\gamma}) \ell + S_\beta C_{\alpha-\gamma} d \\ C_\alpha C_{\alpha-\gamma} \ell - C_\beta (C_\gamma - C_\alpha C_{\alpha-\gamma}) \ell + S_\beta S_{\alpha-\gamma} d \\ C_\beta d + S_\alpha S_\beta \ell \end{bmatrix} \quad (\text{Eq. 7})$$

The pointing position Pt is derived by translating P'' to  $\Sigma_1$ .

$$\mathbf{P}_t = \begin{bmatrix} C_\phi & -S_\phi & 0 \\ S_\phi & C_\phi & 0 \\ 0 & 0 & 1 \end{bmatrix} \cdot \begin{bmatrix} C_\theta & 0 & S_\theta \\ 0 & 1 & 0 \\ -S_\theta & 0 & C_\theta \end{bmatrix} \cdot \begin{bmatrix} P_1 \\ P_2 \\ P_3 \end{bmatrix} + \begin{bmatrix} X_t \\ Y_t \\ Z_t \end{bmatrix} = \begin{bmatrix} C_\phi (C_\theta P_1 + S_\theta P_3) - S_\phi P_2 + S_\theta C_\phi L \\ S_\phi (C_\theta P_1 + S_\theta P_3) + C_\phi P_2 + S_\theta S_\phi L \\ -S_\theta P_1 + C_\theta P_3 + C_\theta L + L_0 \end{bmatrix} \quad (\text{Eq. 5})$$

Here, the coordinates of P0 are defined as [Xt, Yt, Zt]<sup>T</sup>. Finally, Pt is translated to the global coordinate

by using the position of the Total Station and the rotation angle around the axis Z0 measured in the initialize mode.

### 3.5 Device Configuration

The prototype of the pointing device is shown in Figure 8. The length of  $\ell$  is 1000 millimeters and the ribs are assembled on the bar to suppress deflection. The microprocessor calculates the three angles mentioned above with the output of the sensors. It also sends control commands (device search and measurement) to the host PC via Bluetooth modem, and measurement data are sent between the two sides.

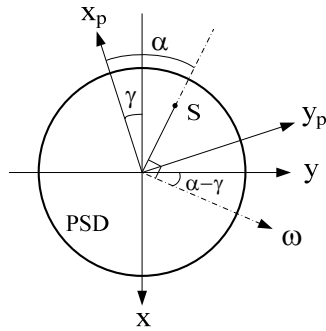


Figure 7 Transform by  $\alpha$  and

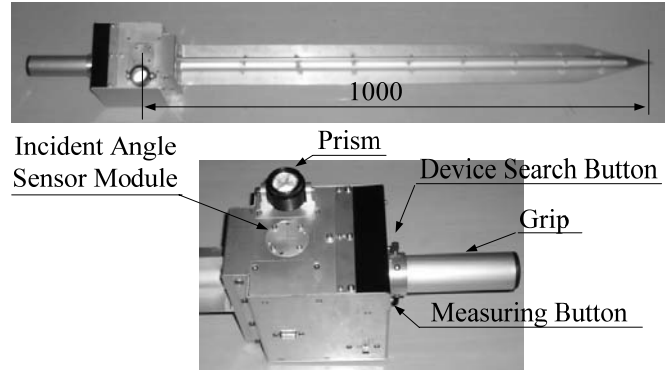


Figure 8 Pointing Device

The prism is mounted on the receiving surface to be found by the total station.

## 4. Positioning Device

### 4.1 Theory of Positioning

This system has a positioning device for accurate positioning and marking. We produced a prototype for use on the floor and on machine foundations. As shown in Figure 9, the laser is irradiated to a different point  $P'$  from the target  $P$  because of the level difference in the case of the positioning on the floor. In use, the operator sets the device after irradiation and measures the horizontal distance  $L_0$ , from the total station to the prism. The operator measures the horizontal distance  $L_1$  from the prism to the target point and then measures  $L_1$  with the device and marks.

### 4.2 Device Configuration

The prototype of the positioning device is shown in Figure 10. It consists of the prism, axial slider, scale, slit, screws and level. The level of the device is adjusted via the screws and the axial direction via referring to the laser through the slit and the vertical line on the slider. The slider is moved along the scale for positioning and the operator makes marking with a pen through the hole on the slider.

## 5. Results of Experiments

### 5.1 Conditions of Experiments

We conducted experiments to evaluate the measuring accuracy of the prototype system. The experimental field is about 5 meters wide and 12 meters long. It is an indoor field and is not subjected to direct sunlight. The reference values for evaluation are measured with the two transits set on the reference points. The transit is NET 2000 products produced by SOKIA and the angle resolution is 2 seconds. The target accuracy setting of this system is 5 millimeters at 10 meters from the total station.

### 5.2 Results of Experiments

#### 5.2.1 Position Measurement Mode

The measurement points  $P_1$  and  $P_2$  are set on the floor. Here,  $P_1$  and  $P_2$  are defined on each coordinate system, and as shown in Figure 11.  $S_1$  and  $S_2$  are the reference points of each coordinate system and the position of the two transits. The position of the total station is measured by the transits as  $T_1(2399.5,$

8384.3, 1424.8) on  $\Sigma_{01}$  and T2(2340.7, 5082.1, 1425.1) on  $\Sigma_{02}$ . The evaluation is done in six cases of the device posture as shown in Figure 12. The posture which is set on the measurement points at reasonable angle is defined as the default, and it's changed to the six cases while the tip is kept to set on the points.

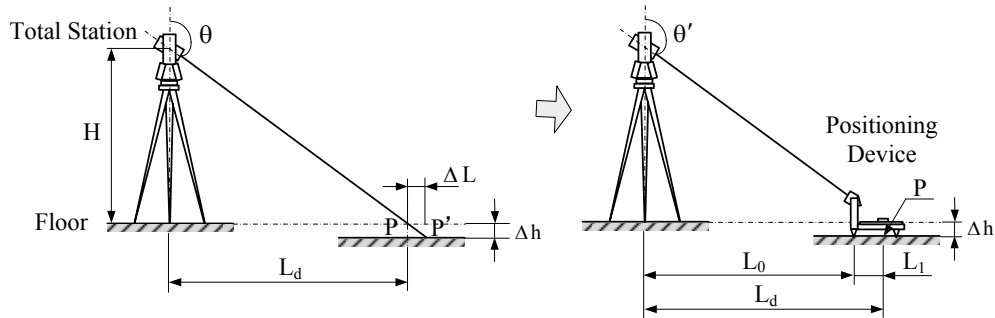


Figure 9 Theory of Positioning

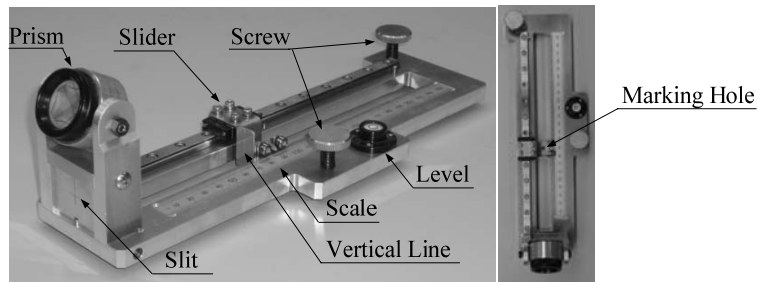


Figure 10 Positioning Device

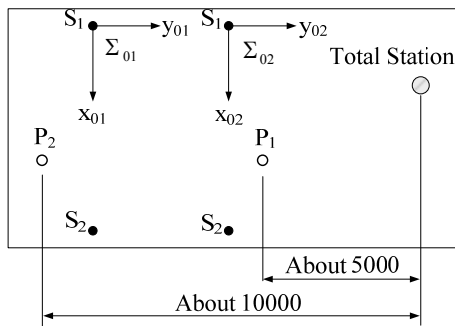


Figure 11 Experiment Field and Setting

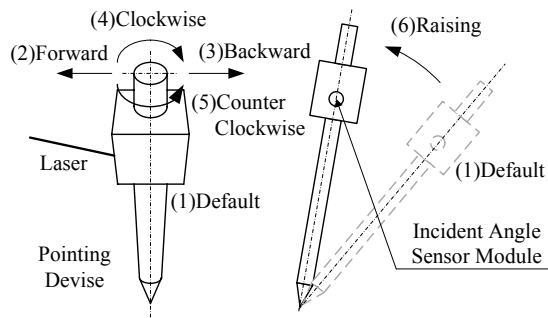


Figure 12 Posture of Pointing Device of Measurement Mode

The results are shown in Table 1. The measurement errors are evaluated as the differences from the results measured by the transits and expressed as the root sum square of each coordinate error. They are less than 5 millimeters on both points except for the one case of (6) at P1. It is supposed that the error is from the measurement accuracy of the sensors, especially the incident angle sensor module. It is considered to be necessary to analyze laser behavior in the incident angle sensor module and to improve the calibration equipment for accuracy and repeatability.

## 6. Conclusions

We have proposed a 3D measuring system for application in the construction field, especially for equipment work. In this paper, we presented a prototype of the system and the results of the experiments to evaluate the accuracy of measurements. The results of experiments demonstrated that the accuracy of position measurement with the pointing device is approximately 5 millimeters and the accuracy of positioning with the positioning device is approximately 2 millimeters. In the future, we will analyze the laser

behavior and reconsider the configuration of the incident angle sensor and the method of the calibration to improve the accuracy of measuring with the pointing device. We will also redesign it for reducing the size and weight, and consider the other pointing methods such as the laser. Concerning the positioning device, we will make improvements so that it can be used on walls and ceilings.

Table 1 Results of Point Measurement Mode

		X[mm]	Y[mm]	Z[mm]	Error[mm]	
P <sub>1</sub>	Result by Transits	3192.8	3539.9	5.5		
	Result by the System at Each of the Six Postures	(1)	3192.3	3542.2	4.7	2.5
		(2)	3192.0	3537.6	4.9	2.5
		(3)	3192.3	3543.1	5.0	3.3
		(4)	3192.3	3537.4	4.9	2.6
		(5)	3192.4	3538.9	4.9	1.2
		(6)	3191.9	3545.8	3.7	6.2
P <sub>2</sub>	Result by Transits	3262.8	-4762.0	11.9		
	Result by the System at Each of the Six Postures	(1)	3262.7	-4761.3	10.7	1.4
		(2)	3264.0	-4760.0	10.3	2.8
		(3)	3263.2	-4760.2	11.0	2.1
		(4)	3262.4	-4766.6	11.0	4.7
		(5)	3261.6	-4763.1	9.0	3.3
		(6)	3262.2	-4761.3	10.6	1.6

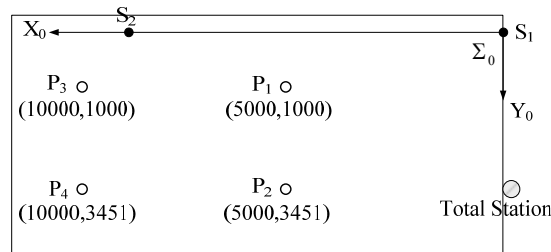


Figure 13 Experiment Field and Setting of Positioning Mode

Table 2 Results of Positioning Mode

Point	No.	X [mm]	Y [mm]	Error [mm]		
				E <sub>x</sub>	E <sub>y</sub>	RSS
P <sub>1</sub>	1	4998.7	1000.1	-1.3	0.1	1.3
	2	4999.3	999.8	-0.7	-0.2	0.7
	3	4999.3	1000.3	-0.7	0.3	0.8
P <sub>2</sub>	1	5000.0	3450.6	0.0	-0.4	0.4
	2	5000.1	3450.9	0.1	-0.1	0.1
	3	4999.9	3450.7	-0.1	-0.3	0.3
P <sub>3</sub>	1	9998.9	998.1	-1.1	-1.9	2.2
	2	9998.9	998.1	-1.1	-1.9	2.2
	3	9998.8	998.2	-1.2	-1.8	2.2
P <sub>4</sub>	1	10000.0	3448.9	0.0	-2.1	2.1
	2	10000.1	3448.8	0.1	-2.2	2.2
	3	10000.0	3449.1	0.0	-1.9	1.9

**References**

- [1] Ward, A., and et al. (1997). "A New Location Technique for the Active Office", IEEE Personal Communications, Vol.4, No.5, pp.42-47.
- [2] Kien, D. T., and et al. (2002). "Un ultrasonic Indoor Positioning System with Self-Configuration", Proceeding of IEICE General Conference, pp.243
- [3] Pedrovski, I., et al., (2004) "Pseudolite Application for ITS", Technical Report of IEICE, pp.13-18.
- [4] Kawamura, K., (2006) "Engineering Process Innovation by 3D Laser Scan", Journal of Japan Society for Design Engineering, pp.83-87.
- [5] Ohtsu, S., et al., (2007) "Method of processing data with a cloud of points on the 3-D shape surveying", Journal of applied computing in civil engineering, Vol.16, pp. 27-36